ADVANCED MATERIALS

DOI: 10.1002/adma.200502770

Nanostructuring and High Thermoelectric Efficiency in p-Type $Ag(Pb_{1-y}Sn_y)_mSbTe_{2+m}$**

By *John Androulakis*, *Kuei Fang Hsu*, *Robert Pcionek*, *Huijun Kong*, *Ctirad Uher*, *Jonathan J. D'Angelo*, *Adam Downey*, *Tim Hogan*, and *Mercouri G. Kanatzidis**

Thermoelectric (TE) power generation has come to be appreciated as an attractive means of low-cost conversion of waste heat to useful electrical energy with a small environmental impact. For a compound to qualify as an efficient thermoelectric material it should exhibit the highest TE figure of merit, ZT, possible at the temperature of operation, T. ZT is defined as

$$ZT = \frac{S^2\sigma}{\kappa}T \quad (1)$$

and it involves the simultaneous manipulation of the TE power (absolute Seebeck coefficient) S, the electrical conductivity σ, and the thermal conductivity κ.

The search for efficient TE materials mainly focuses on degenerate semiconductors since the underlying physics of these systems allow the coexistence of high thermopower values with high electrical conductivity to achieve high power factors: $PF = S^2\sigma$. The Seebeck coefficient is inversely related to the electrical conductivity according to the Boltzmann transport equation, and, as a result, maximization of one cannot be achieved without minimization of the other. An interesting alternative that has been recently suggested to achieve high power factors is the quantum-confinement effect; however, definite experimental verification of this is still lacking.[1]

Another route to achieving high-performance TEs is through the minimization of the thermal conductivity. To this end, many suggestions have been made to increase ZT. These include the phonon-glass electron-crystal approach[2] (where loosely bound atoms rattle in cage structures[3]) as in clathrates,[4] and the thin-film multilayer approach where the introduction of interfaces significantly reduces phonon propagation.[5] Indeed, artificial thin-film superlattice structures grown by molecular-beam epitaxy (MBE) like Bi_2Te_3/Sb_2Te_3[6] and $PbSe_{0.98}Te_{0.02}$/PbTe[7–9] exhibit very low thermal conductivities and, as a result, enhanced ZT values. The key feature of these systems is the large number of interfaces introduced by the inherent nanofabrication technique that in turn reduce the phononic part of κ through interface phonon scattering. Interestingly, "nanocomposites" in bulk form have been recently identified in the n-type $AgPb_mSbTe_{2+m}$ systems[10] where compositional fluctuations at the nanoscopic level, resulting in a distinct type of nanostructuring, seem to play a key role in the previously reported very low thermal conductivity.[11] In contrast to the thin-film multilayers, bulk nanocomposite systems offer the advantages of large-scale industrial production and the sustenance of large thermal gradients for extended time. The challenge, therefore, lies in identifying equally efficient p-type materials so that they can be employed in the fabrication of TE modules.

Here we report on the $Ag(Pb_{1-y}Sn_y)_mSbTe_{2+m}$ series and show that certain compositions exhibit high performance p-type TE properties (e.g., $ZT \sim 1.45$ at 630 K) as a result of their very low thermal conductivity. We show as well that the $Ag(Pb_{1-y}Sn_y)_mSbTe_{2+m}$ systems are in fact bulk nanocomposites. We demonstrate that varying the m and y values, as well as the Ag and Sb concentrations, allows for control over a wide range of properties such as carrier concentration, TE power, and thermal conductivity. These exceptional properties, derived from specific compositions, outperform the standard state-of-the-art p-type systems like TAGS ($(AgSbTe_2)_{0.15}(GeTe)_{0.85}$, $ZT \sim 1.2$ at 720 K[12]), PbTe ($ZT \sim 0.7$ at 740 K[13]), and Zn_4Sb_3 ($ZT \sim 1.3$ at 670 K[14]).

The electronic-transport properties of the $Ag(Pb_{1-y}Sn_y)_mSbTe_{2+m}$ system can be tuned primarily through carefully controlling the Pb/Sn ratio, i.e., the y value, and secondarily the Ag and Sb composition. Increasing the Sn concentration results in enhanced electrical conductivity and a subsequent low TE voltage response. On the other hand, we have found that the TE power varies approximately as a linear function of y, and, at 650 K, can be tuned to reach as high as $\sim 280\ \mu V\,K^{-1}$. We find that the functional dependence of the electrical conductivity on temperature does not change dramatically with y or m and scales as T^{-n}, where $1.8 \le n \le 2.25$ from room temperature up to 640 K. Therefore, the electrical conductivity at 600 K is roughly 22–28 % of the room-temperature electrical conductivity for all y. It is important to mention that there was

[*] Prof. M. G. Kanatzidis, Dr. J. Androulakis, Dr. K. F. Hsu, R. Pcionek
Department of Chemistry
Michigan Sate University
East Lansing, MI 48824-1793 (USA)
E-mail: kanatzid@cem.msu.edu
H. Kong, Prof. C. Uher
Department of Physics
University of Michigan
Ann Arbor, MI 48109 (USA)
J. J. D'Angelo, A. Downey, Prof. T. Hogan
Electrical and Computer Engineering Department
Michigan State University
East Lansing, MI 48824-1226 (USA)

[**] We thank Prof. S. D. Mahanti for useful discussions. The 200 kV Field Emission Gun Transmission Electron Microscope was acquired with an NSF grant (DMR-0079578) (MSU Center for Advanced Microscopy). Financial support from the Office of Naval Research (MURI program) is gratefully acknowledged. Supporting Information is available online from Wiley InterScience or from the author.

no clear trend of the TE properties observed as a function of *m*. Finally, for the sake of clarity we emphasize that we have not yet exhaustively studied the effect of Ag and Sb concentrations for a certain *m* and *y*, although it seems that increasing Ag and Sb slightly increases the TE power and reduces the electrical conductivity.

Another interesting feature of the transport properties is the robustness of p-type conductivity. Alloying of SnTe with PbTe makes the solid solution $Pb_{1-x}Sn_xTe$ an n-type material.[15] Although we have tried several *y* values and Ag and Sb concentrations, we always observed p-type behavior. It is evident that the $Ag(Pb_{1-y}Sn_y)_mSbTe_{2+m}$ system has considerable electronic structure differences compared to PbTe.

Figure 1a presents the electrical conductivity and the TE power, respectively, as a function of temperature for $Ag_{0.5}Pb_6Sn_2Sb_{0.2}Te_{10}$. The electrical conductivity has a room-temperature value of 1000 S cm^{-1} and decreases to 200 S cm^{-1} at 700 K following a T^{-2} scaling law (see Fig. 1b). On the basis of Hall effect measurements, the hole mobility in $Ag_{0.5}Pb_6Sn_2Sb_{0.2}Te_{10}$ is calculated to be ~165 cm^2 V^{-1} s^{-1}. Hall effect measurements in the range $4.2 \le T \le 300$ indicated a positive Hall coefficient consistent with thermopower measurements for p-type conductivity. Assuming a simple one-carrier, single-band model, we calculated a carrier concentration of 4×10^{19} cm^{-3}. The carrier concentration can also be tuned through the Pb/Sn ratio and Ag and Sb concentrations. We have observed carrier concentrations as high as 3×10^{20} cm^{-3}.

The Seebeck coefficient of $Ag_{0.5}Pb_6Sn_2Sb_{0.2}Te_{10}$ proves to have a very interesting behavior. At low temperatures the thermopower does not exhibit appreciable values. However, in the temperature range $340 \le T \le 550$ K, the thermopower rapidly increases with temperature, adding almost 160 μV over 200 K. Plotting the natural logarithm of the conductivity ($\ln(\sigma)$) against the measured absolute Seebeck coefficient and taking the slope of the curve we arrive at $\partial S/\partial \ln \sigma \sim 135$ μV K^{-1} change per decade of resistivity (see Fig. 1c). This is larger than the classical result of $\partial S/\partial \ln \sigma \sim k_B/e$ μV K^{-1} (where k_B is the Boltzmann constant and *e* is the charge of the electron) change per decade of resistivity for the diffusive thermopower of a low-carrier-concentration system. As proposed for PbTe, this is likely due to an increasing effective mass with increasing temperature.[16]

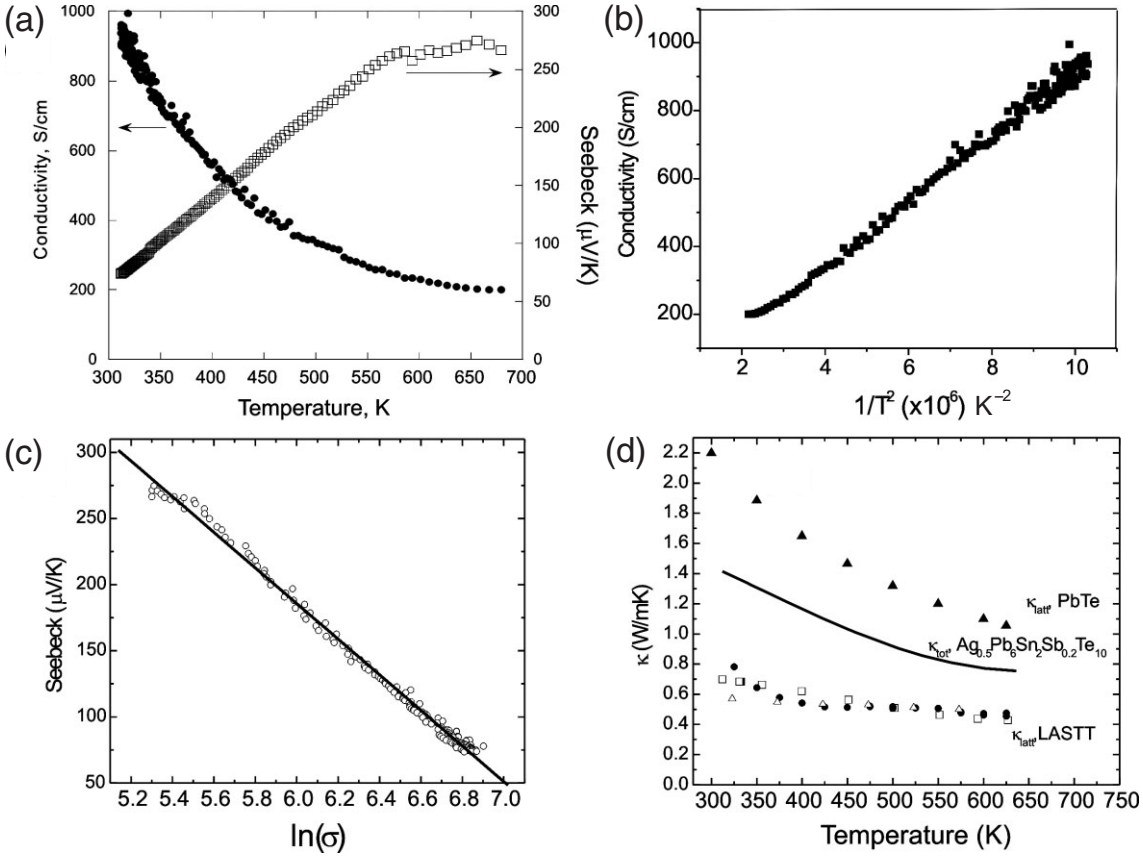

Figure 1. a) Electrical conductivity and absolute Seebeck coefficient as a function of temperature for $Ag_{0.5}Pb_6Sn_2Sb_{0.2}Te_{10}$. b) The characteristic scaling of the conductivity which follows the law $\sigma \sim T^{-2}$. c) Plot of the Seebeck coefficient versus the natural logarithm of the electrical conductivity. The slope of the straight line yields $\partial S/\partial \ln \sigma \sim 135$ μV K^{-1}. d) Lattice thermal conductivity for three compounds of the $Ag(Pb_{1-y}Sn_y)_mSbTe_{2+m}$ series (open squares for $AgPb_{12}Sn_4Sb_{0.4}Te_{20}$, open triangles for $AgPb_{14}Sn_6Sb_{0.4}Te_{24}$, and closed circles for $AgPb_{10}Sn_{10}Sb_{0.67}Te_{22}$) in comparison to that of PbTe. Notably, the lattice thermal conductivity of $Ag(Pb_{1-y}Sn_y)_mSbTe_{2+m}$ is 65–50 % lower than that of PbTe and remains at almost the same value despite differences in Pb/Sn ratio (alloying) and defect concentration. The solid line depicts the total κ of $Ag_{0.5}Pb_6Sn_2Sb_{0.2}Te_{10}$.

ADVANCED MATERIALS

We have measured the thermal conductivity of several compounds within the $Ag(Pb_{1-y}Sn_y)_mSbTe_{2+m}$ series as a function of temperature, combining specific heat measurements with the flash diffusivity method and subtracting the electronic part. (The measured thermal conductivity is the sum of two contributions, namely the lattice part, κ_{latt}, and the electronic part, κ_{el}, which reflects the contribution of the carriers in the heat conduction process. The latter part is quantified through the Wiedemann–Franz law, which simply states that $\kappa_{el} = \sigma T L_o$, where the Lorenz number $L_o = 2.44 \times 10^{-8}\ W\,\Omega\,K^{-2}$). The derived κ_{latt} for $AgPb_{12}Sn_4Sb_{0.4}Te_{20}$ (open squares), $AgPb_{14}Sn_6Sb_{0.4}Te_{24}$ (open triangles), and $AgPb_{10}Sn_{10}Sb_{0.67}Te_{22}$ (filled circles) in comparison with that of PbTe (filled triangles) is depicted in Figure 1d. These same results were repeated several times for different compositions of both m and y. For the sake of simplicity, we have included only three compositions. It can be readily seen that the lattice thermal conductivity of the LASTT (lead, antimony, silver, tin, tellurium) system at room temperature is $\sim 0.70\ W\,m^{-1}\,K^{-1}$, only 40 % that of PbTe, and at 620 K is $\sim 0.43\ W\,m^{-1}\,K^{-1}$, which is ~ 50 % that of PbTe. Our results indicate significant changes in the lattice dynamics of the investigated system at high temperatures deviating from the Debye–Peierls theory, which predicts a scaling law $\kappa_{latt} \sim 1/T$.[13] It is interesting to note that this very low κ_{latt} value is significantly lower that those of either $AgPb_mSbTe_{2+m}$ or $AgSn_mSbTe_{2+m}$ at comparable m values and only twice as large as that observed in the thin-film MBE-grown PbTe superlattices ($\sim 0.33\ W\,m^{-1}\,K^{-1}$).[6]

A high-resolution transmission electron microscopy (HRTEM) investigation of several samples of $Ag(Pb_{1-y}Sn_y)_mSbTe_{2+m}$ revealed striking structural nanoscopic, coherent inhomogeneities (Fig. 2). The localized wavy pattern that is shown in Figure 2 has a lengthscale of ~ 3 nm and appears unambiguously in all the investigated samples. The nanostructure is coherent with its surrounding crystal matrix and is related to compositional fluctuations between Ag, Sb, and Pb/Sn. In other words, Pb/Sn-poor regions are formed that sit in the surrounding matrix endotaxially without disturbing the electronic flow. Other types of nanometer-scale inhomogeneities are observed as well, such as distinct nanocrystals 5–20 nm in size, see Figure 3b. Since there is no observed scaling in κ_{latt}, neither with m and/or y nor with the introduction of point defects, it would appear that strong suppression of the intermediate frequency heat-carrying phonons is achieved via nanostructuring.[15] With decreasing y we also have observed via scanning electron microscopy very small amounts of sporadic tellurium phase in the material, which may manifest itself with some evaporation at high temperature.

Figure 3a presents the obtained ZT values as a function of temperature for a number of LASTT materials with compositions indicated on the graph. The highest ZT achieved so far was ~ 1.45 at 627 K for $Ag_{0.5}Pb_6Sn_2Sb_{0.2}Te_{10}$. It is interesting to point out that at least two samples cross $ZT = 1$ at a temperature below 550 K. These results are very encouraging, and hold promise for a $ZT \sim 2$ in the near future. Figure 3b compares

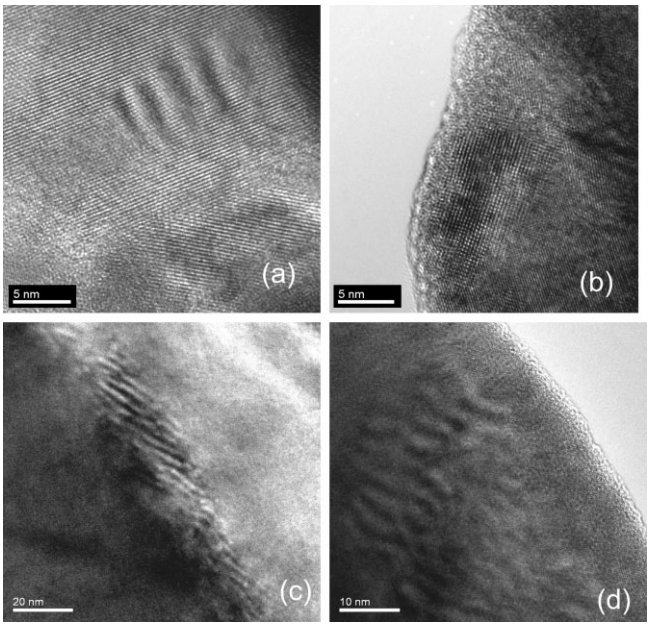

Figure 2. a) HRTEM image of $Ag_{0.5}Pb_6Sn_2Sb_{0.2}Te_{10}$ showing a nanostructure (bright stripes) that is rich in Ag and Sb. b) Characteristic inhomogeneity observed as an embedded nanocrystal 5 nm × 20 nm in size in $Ag_{0.5}Pb_6Sn_2Sb_{0.2}Te_{10}$. c) HRTEM image of $Ag_{0.9}Pb_5Sn_3Sb_{0.7}Te_{12}$. d) Same as (c), but showing compositional waves over an extended region.

the ZTs of some of the compositions of this study with state-of-the-art p-type materials like TAGS and PbTe. Although all the curves start from a very low initial value ($ZT < 0.3$), the $Ag(Pb_{1-y}Sn_y)_mSbTe_{2+m}$ compounds exhibit a steep slope and by 500 K they have already outperformed TAGS.

In summary, we have shown that certain compositions in the p-type system of the formula $Ag(Pb_{1-y}Sn_y)_mSbTe_{2+m}$ outperform all state-of-the-art p-type bulk TE materials. The existence of two chemical "knobs", namely the Pb/Sn ratio and the Ag and Sb concentration, allows for tuning of the electronic-transport properties and therefore the identification of compositions with very high ZTs, the highest being ~ 1.45 at 627 K. The main advantage of this system is its exceptionally low lattice thermal conductivity. Our experiments showed that the lattice thermal conductivity is not significantly affected by changes in point defects and alloying, therefore relating the suppression of this property primarily to the existence of nanostructures endotaxially embedded in the surrounding matrix.

Experimental

Chemical Synthesis and Material Preparation: The $Ag(Pb_{1-y}Sn_y)_mSbTe_{2+m}$ materials (LASTT = lead, antimony, silver, tin, tellurium) were produced by mixing elemental high-purity starting materials in fused-silica-quartz tubes. The tubes were evacuated, sealed, and fired over a period of 12 h at 1000 °C in a rocking furnace. The melt was held there for 6 h with an intermediate 2 h period of rocking before being slowly cooled to room temperature over 48 h. We have synthesized and characterized compositions with $8 \le m \le 36$ and $0.1 \le y \le 0.6$ with a combination of Ag/Sb ratios to achieve the best results. Each

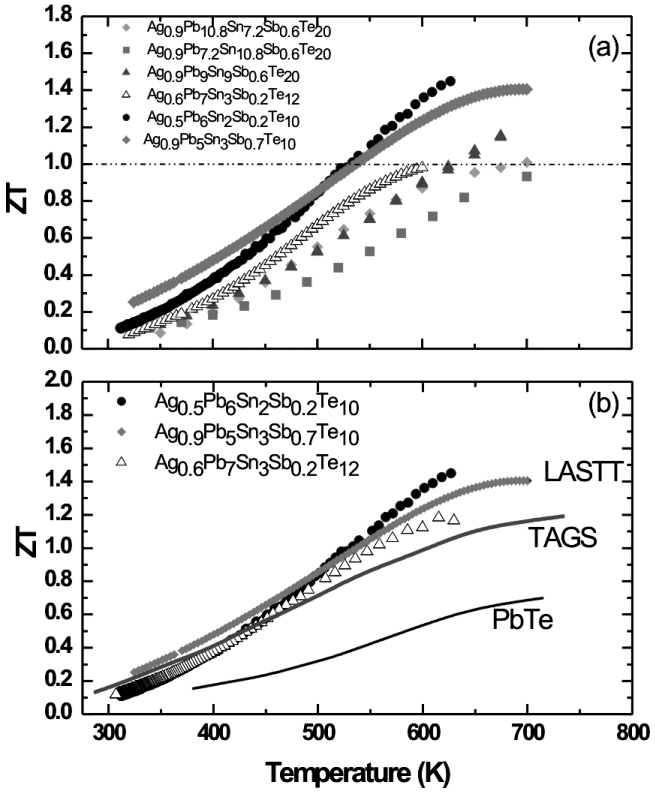

Figure 3. a) The TE figure of merit, *ZT*, as a function of temperature for a number of compounds of the $Ag(Pb_{1-y}Sn_y)_mSbTe_{2+m}$ series as indicated on the graph. Notice that all the compounds have reached $ZT=1$ by 700 K, while chemical tuning allows for the realization of compounds that surpass $ZT=1$ at 520 K. The maximum *ZT* achieved so far is 1.45. b) Comparison of the figures of merit as a function of temperature for some of the best LASTT samples (indicated on the graph), with two of the state-of-the-art p-type TEs, TAGS (tellurium antimony germanium silver: AgSbTe2/GeTe solid solution) and PbTe.

produced ingot was cut into three to four slabs (depending on the initial load) of ~0.6–0.9 cm thickness, out of which rectangular-shaped pieces with typical dimensions 0.3 cm × 0.3 cm × 0.6 cm were characterized separately. We did not observe significant differences in the physical properties of specimens from the same ingot.

Structural and Compositional Analysis: Analysis of powder X-ray diffractograms obtained from the produced ingots were always indicative of a single-phase cubic, NaCl-like structure, with lattice parameters varying smoothly with *m* and *y*. Quantitative microprobe analyses of the produced compounds were performed with a JEOL JSM-35C scanning electron microscope equipped with a Tracor Northern EDS detector. Data were acquired using an accelerating voltage of 20 kV and an average accumulation time of 40 s. The results were in excellent agreement with the nominal compositions of the ingots. Therefore, the $Ag(Pb_{1-y}Sn_y)_mSbTe_{2+m}$ materials were chemically homogenous regardless of *m* and *y*. The structural properties of the investigated compounds were examined with a JEOL-2200FS high-resolution field-emission transmission electron microscope attached to a Gatan image filter.

High-Temperature Charge-Transport Measurements: Full details regarding the measurement apparatus used to determine the high temperature electrical conductivity and absolute Seebeck coefficient can be found elsewhere [17].

Low-Temperature Charge and Thermal-Transport Measurements: The Hall effect was measured using a Linear Research AC bridge with 16 Hz excitation in a magnet cryostat capable of fields up to 5 T. Seebeck coefficients and thermal conductivities below 300 K were determined using a longitudinal steady-state technique in a cryostat equipped with two radiation shields. Thermal gradients were measured with the aid of fine Au/Fe-Chromel thermocouples, and a miniature strain gauge served as a heater. For Seebeck probes, we used fine copper wires that had been previously calibrated, and their thermopower contribution had been subtracted from the measured sample thermopower. Radiation losses were experimentally determined in a subsequent measurement where the sample was detached from the sink and suspended by its connecting leads under vacuum. Heater power was carefully adjusted until the thermocouples read the average temperature as in the actual experiment.

High-Temperature Thermal-Conductivity Measurements; The Flash Diffusivity-Specific Heat Method: In the flash method, the front face of a small disc- or square-shaped sample was subjected to a high-intensity, short-duration light pulse, e.g., a laser beam, and the resulting rear-face temperature rise was recorded and analyzed. The thermal diffusivity was determined by the shape of the temperature-versus-time curve at the rear face. The thermal diffusivity of our samples was determined at the Thermophysical Properties Research Laboratory (TPRL Inc., Lafayette, IN). The specific heat of our samples in the range $300 \le T \le 800$ K was determined at TPRL Inc. and at Michigan State University with a Shimadzu DSC-50 differential scanning calorimeter in reference to the specific heat of a sapphire standard sample using Al sample containers. The heat capacities of the sample containers were also measured and carefully extracted. X-ray spectroscopic analysis of the samples after the end of the experiments did not show Al contamination.

The thermal conductivities of the samples were determined by the relationship $\kappa = C_p \lambda d$, where C_p is the specific heat, λ is the thermal diffusivity, and *d* is the density of the sample.

Received: December 31, 2005
Published online: April 6, 2006

[1] L. D. Hicks, T. C. Harman, X. S. Sun, M. S. Dresselhaus, *Phys. Rev. B: Condens. Matter Mater. Phys.* **1996**, *53*, R10493.
[2] G. A. Slack, in *CRC Handbook of Thermoelectrics* (Ed: D. M. Rowe), CRC Press, Boca Raton, FL **1995**.
[3] B. C. Sales, D. Mandrus, R. K. Williams, *Science* **1996**, *272*, 1325.
[4] B. C. Sales, B. C. Chakoumakos, D. Mandrus, J. W. Sharp, *J. Solid State Chem.* **1999**, *146*, 528.
[5] T. C. Harman, P. J. Taylor, M. P. Walsh, B. E. LaForge, *Science* **2002**, *297*, 2229.
[6] R. Venkatasubramanian, E. Siivola, V. Colpitts, B. O'Quinn, *Nature* **2001**, *413*, 597.
[7] T. C. Harman, D. L. Spears, M. J. Manfra, *J. Electron. Mater.* **1996**, *25*, 1121.
[8] H. Beyer, J. Nurnus, H. Böttner, A. Lambrecht, T. Roch, G. Bauer, *Appl. Phys. Lett.* **2002**, *80*, 1216.
[9] T. C. Harman, M. P. Walsh, B. E. Laforge, G. W. Turner, *J. Electron Mater.* **2005**, *34*, L12.
[10] K. F. Hsu, S. Loo, F. Guo, W. Chen, J. S. Dyck, C. Uher, T. Hogan, E. K. Polychroniadis, M. G. Kanatzidis, *Science* **2004**, *303*, 818.
[11] F. D. Rosi, E. F. Hockings, N. E. Lindenblad, *RCA Rev.* **1961**, *22*, 82.
[12] C. Wood, *Rep. Prog. Phys.* **1988**, *51*, 459.
[13] J. M. Ziman, *Electrons and Phonons: The Theory of Transport Phenomena in Solids*, Clarendon, Oxford, UK **1960**.
[14] G. J. Snyder, M. Christensen, E. Nishibori, T. Caillat, B. B. Iversen, *Nat. Mater.* **2004**, *3*, 458.
[15] D. Li, S. T. Huxtable, A. R. Abramson, A. Majumdar, *J. Heat Transfer* **2005**, *127*, 108.
[16] I. Ravich, B. A. Efimova, I. A. Smirnov, in *Semiconducting Lead Chalcogenides*, Plenum, New York **1970**, p. 153.
[17] S. Loo, J. Short, K. F. Hsu, M. G. Kanatzidis, T. Hogan, *Mat. Res. Soc. Symp. Proc.* **2003**, *793*, 375.

